Origin and stability of dark pulse Kerr combs in normal dispersion resonators

Pedro Parra-Rivas[1,2], Damià Gomila[2], Edgar Knobloch[3], Stéphane Coen[4] and Lendert Gelens[1,5,6]
[1] *Applied Physics Research Group, Vrije Universiteit Brussel, 1050 Brussels, Belgium*
[2] *IFISC institute (CSIC-UIB), Campus Universitat de les Illes Balears, E-07122 Palma de Mallorca, Spain*
[3] *Department of Physics, University of California, Berkeley CA 94720, USA*
[4] *Dodd-Walls Centre, and Physics Department, The University of Auckland, Private Bag 92019, Auckland 1142, New Zealand*
[5] *Laboratory of Dynamics in Biological Systems, KU Leuven, Department of Cellular and Molecular Medicine, University of Leuven, B-3000 Leuven, Belgium*
[6] *Department of Chemical and Systems Biology, Stanford University School of Medicine, Stanford CA 94305-5174, USA* *
(Dated: February 24, 2016)

We analyze dark pulse Kerr frequency combs in optical resonators with normal group-velocity dispersion using the Lugiato-Lefever model. We show that in the time domain these correspond to interlocked switching waves between the upper and lower homogeneous states, and explain how this fact accounts for many of their experimentally observed properties. Modulational instability does not play any role in their existence. Furthermore, we provide a detailed map indicating where stable dark pulse Kerr combs can be found in parameter space, and how they are destabilized for increasing values of frequency detuning.

arXiv:1602.07068v1 [nlin.PS] 23 Feb 2016

Optical frequency combs generated in passive Kerr microresonators have attracted a lot of interest in recent years for their potential for on-chip integration of frequency comb technology [1–6]. Their applications span arbitrary waveform synthesis [5], telecommunications [7], and ultra-accurate clocks [4]. These so-called "Kerr frequency combs" (KFCs) are obtained by driving a high-Q microresonator with a continuous-wave (cw) laser. This leads to the generation of spectral sidebands through modulational instability (MI) and subsequent cascaded four-wave mixing. Interestingly, much can been learned about KFCs by considering a time domain representation. In fact, most reported KFCs correspond either to extended periodic patterns or to ultrashort pulses known as temporal cavity solitons (CSs), stable or fluctuating [8–14]. These studies have benefitted from the fact that KFCs can be modeled using a simple mean-field equation, the Lugiato-Lefever equation (LLE) [9, 15].

The bulk of KFC studies so far deals with microresonators exhibiting *anomalous* second-order group velocity dispersion (GVD) at the pump wavelength. However, due to the difficulty in obtaining anomalous GVD in some spectral ranges, generation of KFCs from normal GVD microresonators is now also being sought and has recently been achieved experimentally by several groups [16–18]. In [18], a full time-domain characterization is reported: the field is found to consist of square dark pulses of different widths — low intensity dips embedded in a high intensity homogeneous background — with a complex temporal structure. These observations match several previous numerical predictions [14, 16, 19–21] and are in stark contrast with the isolated ultrashort bright localized structures observed with anomalous GVD [8, 12].

There has been some speculation as to the physical origin of the temporal structures observed in normal GVD KFCs, which have been called platicons, dark pulse KFCs, or dark CSs [18, 21]. To clarify this issue, we present here a detailed bifurcation analysis of dark structures in the LLE with normal GVD, and predict their region of existence and stability. In particular, we clearly show that they are intimately related to so-called switching waves (SWs) — traveling front solutions of the LLE that connect the upper and lower homogenous state solutions. These SWs were studied theoretically in the 80s [22] and their temporal dynamics were observed experimentally in fiber resonators in the 90s [23]. The role of fronts in normal GVD KFCs is briefly suggested in [18, 21], but in fact it is so central to the stability of the dark structures that the term platicon does not really capture their essence. In this Article, we therefore prefer to employ the terminology of dark pulse KFCs.

We start our analysis from the LLE, which was originally introduced in optics in the context of transverse resonators [24]. Using the normalization of [8], the LLE reads

$$\partial_t u = -(1+i\theta)u + i|u|^2 u + u_0 - i\partial_\tau^2 u\,, \qquad (1)$$

where t is the slow time describing the evolution of the intracavity field $u(t,\tau)$ on the time scale of the cavity photon lifetime, while τ is the fast time that describes the temporal structure of that field on the time scale of a resonator roundtrip L. The first term on the right-hand side describes cavity losses (the system is dissipative by nature); θ measures the cavity detuning between the frequency of the driving field and the nearest cavity resonance; the cubic term represents the (self-focusing) Kerr nonlinearity; u_0 is the amplitude of the homogeneous (cw) driving field or pump; and the fast-time derivative models GVD, here assumed normal at the pump frequency and limited to second order. In this form, the LLE has only two control parameters: θ and u_0.

* lendert.gelens@kuleuven.be

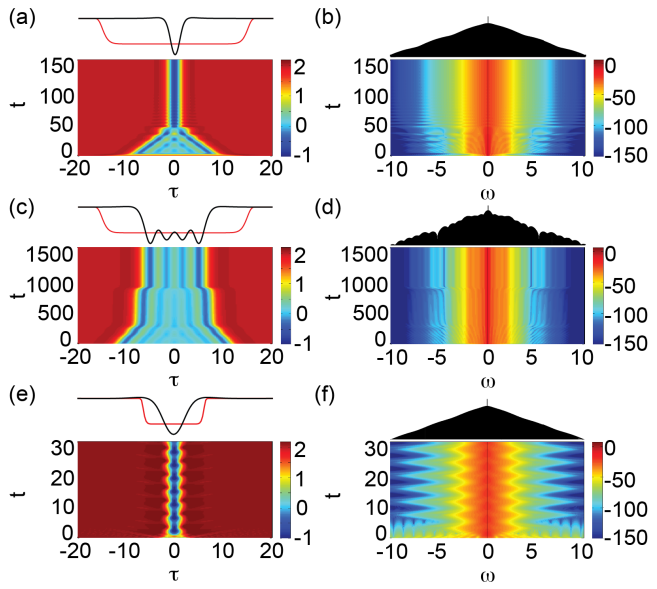

FIG. 1: Evolution of the temporal structure [left; Re(u)] and corresponding spectral intensity (right; in dB) of an initial broad dark pulse over successive roundtrips represented as color density plots for (a,b) $(\theta, u_0) = (4, 2.25)$, (c,d) $(\theta, u_0) = (4, 2.18)$, (e,f) $(\theta, u_0) = (5, 2.6)$. The red (black) curves above the plots correspond to the initial (final) profiles.

To illustrate our discussion, we first present in Fig. 1 typical dark pulse KFC dynamics both in the temporal (left) and spectral (right) domains. In each case, the initial condition (red curve atop each left plot) is a broad dip of depth 2 in the upper homogeneous solution. In (a),(b) and (c),(d) we use the same detuning $\theta = 4$ and initial condition but slightly different driving amplitude u_0 (as listed in the caption). In both cases the initial broad dip shrinks in time, eventually coming to a halt and forming a stable dark pulse KFC. The final dark temporal structures (black curve atop each plot) are markedly different, however, one being broader and far more complex than the other. Fig. 1(c) also reveals the intermediate existence of an even broader structure. Next, Figs. 1(e),(f) illustrate a simulation with an increased detuning, $\theta = 5$. The system again evolves to a dark pulse KFC, but it is no longer stable: it oscillates (breathes) in time. From these simulations, several conclusions can be drawn about dark pulse KFCs (Refs. [14, 18, 21] also mention these features): (i) they exist in the LLE with normal GVD and form as a dip in a background of higher intensity; (ii) they can have very different widths; and (iii) they can undergo dynamical instabilities such as breathing. In what follows, it is our goal to describe and explain all these different features and provide a map showing where the different solutions exist in the parameter space (θ, u_0).

We start by providing a clear definition of a dark CS

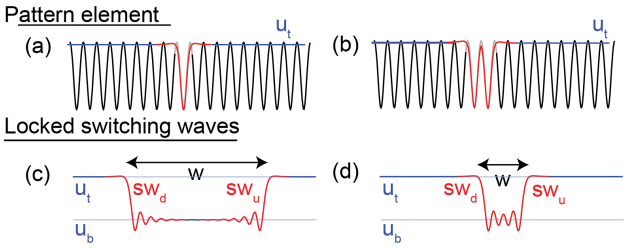

FIG. 2: Sketch of two different scenarios for dark pulse KFCs (in the time domain). (a),(b) *Pattern element*: a connection between the high intensity homogeneous solution u_t and the periodic pattern. (c),(d) *Locked SWs*: the high (u_t) and low (u_b) intensity homogeneous solutions form a stable connection.

or dark pulse KFC and establishing the basic requirements for their formation. Figs. 2(a),(b) sketch in the time domain the first scenario (in red): a stable homogeneous steady state (HSS) solution of high intensity u_t (in blue) and a stable periodic pattern generated at MI (in black) coexist and form a connection. As indicated, this connection can include one oscillation of the pattern (a), two oscillations (b), or more. We refer to this type of dark pulse KFC as a *pattern element*. However, this type of connection does not appear to exist in Eq. 1, despite the coexistence between a stable HSS and a periodic pattern for $\theta > 2$ [25]. In contrast, such localized solutions are present in LLE with anomalous GVD (albeit involving the *low* intensity HSS u_b rather than the high intensity HSS u_t) and explain the presence of the typical bright temporal CSs that are observed in this case [8, 10, 13, 14]. In the presence of higher order GVD, the LLE with anomalous GVD can also admit a stable high intensity HSS and a periodic pattern, allowing dark CSs to exist as pattern elements [26].

Figs. 2(c),(d) demonstrate a second scenario for a dark pulse KFC. Whenever two HSSs coexist, which occurs in Eq. (1) for $\theta > \sqrt{3}$, and are both stable, which occurs with normal GVD [25], the high (u_t) and low (u_b) intensity HSSs (in blue) can connect to one another through what are called *switching waves* (SWs) or fronts [22, 23, 27]. When these SWs (sw_d and sw_u in red) interlock stably, a dark temporal structure of width w is formed. This is the type of dark pulse KFC observed in microresonators with normal GVD.

To understand how such combinations of SWs arise and are stable, let us discuss the properties of individual SWs in more detail (see also [22, 23, 27]). Fig. 3(a) shows the temporal profile $|u(\tau)|$ of a typical SW sw_d for $(\theta, u_0) = (4, 2.175)$. The profile is asymmetric: sw_d leaves the top HSS u_t monotonically, but approaches the bottom HSS u_b in an oscillatory way. Close to u_b, this oscillatory approach can be approximated linearly in the form $sw_\mathrm{d}(\tau) - u_\mathrm{b} \propto e^{\lambda\tau}$. Here $\lambda = q + i\Omega$ is a complex eigenvalue, with q the damping rate of the oscillations and Ω their frequency. Figs. 3(b),(c) illustrate how the

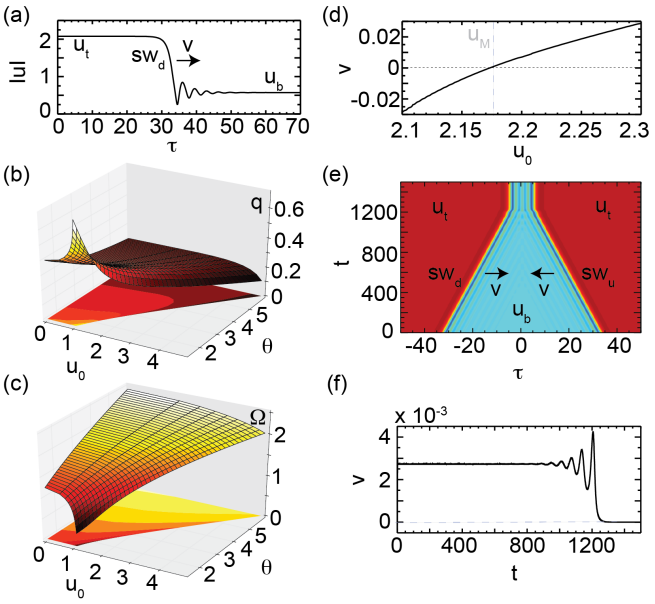

FIG. 3: (a) Temporal profile of $sw_{\rm d}$ for $(\theta, u_0) = (4, 2.175)$. (b,c) Damping rate q and frequency Ω of the oscillatory tail near $u_{\rm b}$ as a function of (θ, u_0). (d) Velocity of $sw_{\rm d}$ versus driving amplitude u_0 for $\theta = 4$. (e) Temporal evolution of two SWs, $sw_{\rm d}$ and $sw_{\rm u}$, approaching each other [density plot of Re(u)] and (f) the corresponding velocity of $sw_{\rm d}$ over time.

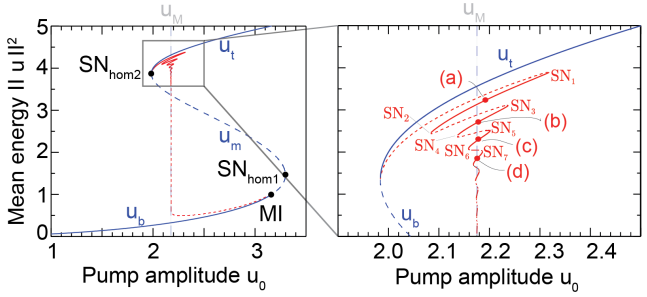

FIG. 4: Bifurcation diagram of dark pulse KFCs (red) for $\theta = 4$, with a zoom (right) of the bifurcation branches close to the top HSS u_t. Stable (unstable) structures are indicated using solid (dashed) lines. Blue lines correspond to HSSs.

eigenvalues, and thus the profile of the SW, change with the parameters (θ, u_0). See [28, 29] for more details on such eigenvalue analysis. The SW generally moves (in the reference frame of the driving field) with a velocity v that depends on the driving amplitude u_0 [see Fig. 3(d)]; $v = 0$ for only one particular value of the driving amplitude, $u_0 = u_{\rm M}$, known as the *Maxwell point* (for $\theta = 4$, $u_{\rm M} \approx 2.175$). The reason the SW moves can be intuitively understood as follows. Above the Maxwell point, the system is comparatively closer to up-switching, thus $u_{\rm b}$ is less favorable, and $u_{\rm t}$ invades $u_{\rm b}$. The opposite occurs below the Maxwell point. Given these properties, it may seem that a stable dark pulse KFC made up of two SWs can only exist at the Maxwell point where the domains do not invade each other. However, away from $u_{\rm M}$, as the SWs set into motion, their oscillatory tails may become interlocked, as in other types of soliton bound states [27, 30–34]. This is illustrated in Figs. 3(e),(f): two SWs initially move towards each other at fixed mean velocity, invading the $u_{\rm b}$ domain, but the overlapping oscillatory tails provide a counteracting force that modulates their velocity, eventually bringing them to a halt and creating a stable dark pulse KFC. Dark pulse KFCs can thus exist provided the velocity of the SWs is small enough to be balanced by the oscillations in the SW tails. Note that the monotonic behavior of the SWs near $u_{\rm t}$ prevents "bright" combinations.

Fig. 4 shows the bifurcation diagram of the dark pulse KFCs (in red) obtained by numerical continuation. The figure shows, in blue, the top ($u_{\rm t}$), middle ($u_{\rm m}$), and bottom ($u_{\rm b}$) HSSs: these are solutions of $I_{\rm t,m,b}^3 - 2\theta I_{\rm t,m,b}^2 + (1+\theta^2) I_{\rm t,m,b} = u_0^2$, where $I_{\rm t,m,b} \equiv |u_{\rm t,m,b}|^2$. These three solutions only exist for $\theta > \sqrt{3}$, and the transitions between them occur via two saddle-node bifurcations $\mathrm{SN}_{\rm hom,1}$ and $\mathrm{SN}_{\rm hom,2}$. The diagram shows that unstable dark KFCs originate from $\mathrm{SN}_{\rm hom,2}$ and that as u_0 increases their mean energy $||u||^2 \equiv L^{-1}\int_0^L |u|^2\, d\tau$ grows until SN_1, a saddle-node bifurcation at which they acquire stability. The temporal profile on the resulting segment of stable dark solitons is shown in Fig. 5(a). These KFCs lose stability at SN_2 but start to develop an additional oscillation in the center. Solutions of this type become stable at SN_3; an example of the resulting stable double-oscillation dark pulse KFC can be found in Fig. 5(b). This process repeats in such a way that between successive saddle-nodes on the left or right a new oscillation period is inserted in the center of the dark structure, resulting in a structure that is temporally broader but less energetic [see Figs. 5(c),(d)].

An additional feature of this snaking branch of solutions is that after each successive turn the range of driving amplitudes over which the branch of solutions exists becomes narrower. In other words, the temporally broader the dark pulse KFC is (or equivalently, the more oscillations it has), the narrower its range of existence. This type of organization is thus appropriately referred to as *collapsed snaking*. This collapse originates in the exponential damping of the oscillations of the SWs: As the distance between $sw_{\rm u}$ and $sw_{\rm d}$ increases, the oscillations rapidly become too weak to be able to compensate the inherent velocity of the SWs. Therefore, very temporally broad dark pulse KFCs can only exist at the Maxwell point $u_{\rm M}$.

The organization of dark pulse KFCs in a collapsed snaking structure strongly suggests that the narrowest dark pulse KFCs should be the most frequent occurrence in experiments. Although this is true for a wide range of

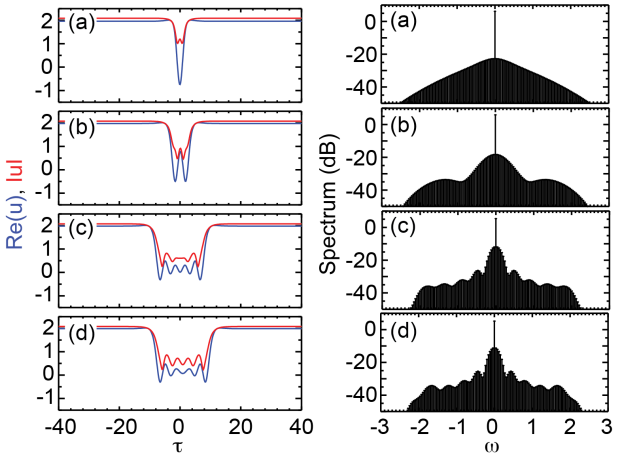

FIG. 5: Temporal profiles [left; Re(u) in blue, $|u|$ in red] and spectral intensities (right, in dB) of dark pulse KFCs corresponding to the locations (a)–(d) in Fig. 4.

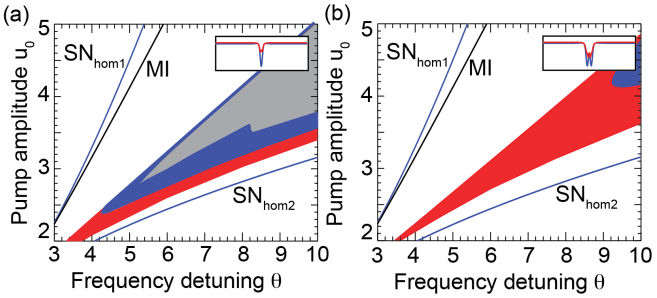

FIG. 6: Regions of existence in the (θ, u_0) parameter space of (a) the single- and (b) the double-oscillation dark KFC. The red (blue) region corresponds to stable stationary (oscillatory) dark KFCs, while within the gray region dark KFCs are unstable and relax to the HSS after a chaotic transient.

parameter values, this statement requires modification as the detuning θ increases, because dark pulse KFCs can then undergo a wide range of instabilities similar to those of bright CSs in the case of anomalous GVD [10, 13]. In Figs. 1(e),(f), we already saw one example of an unstable (breathing) dark pulse KFC. We have explored these instabilities further and Fig. 6 shows stability maps of (a) single-oscillation and (b) double-oscillation dark pulse KFCs. Examples of their temporal profiles, corresponding to Figs. 5(a),(b), are shown in insets. As a reference, we plot the $SN_{\mathrm{hom},1}$, $SN_{\mathrm{hom},2}$, and MI bifurcation lines because dark pulse KFCs can only exist between the $SN_{\mathrm{hom},2}$ and MI lines where u_{t} and u_{b} are both stable (Fig. 4). The red regions in Fig. 6 show the parameter values for which single-oscillation and double-oscillation dark pulse KFCs can be found and are stable. Although the region of existence of dark pulse KFCs shrinks as they become temporally broader (increasing the number of oscillations), the range of stable KFCs is broader for broader KFCs: the stable red region is larger for the double-oscillation KFC than the single-oscillation KFC. In fact dark pulse KFCs with three or more oscillations are stable across their whole region of existence at least up to values of the detuning as high as 10 (not shown here).

As shown in Figs. 1(e),(f), for $(\theta, u_0) = (5, 2.6)$ the single-oscillation KFC is no longer stationary, but instead breathes in time with a well-defined period and amplitude. Such breathers are found throughout the blue regions in Fig. 6. Within the blue region, but close to the gray region, period doubling occurs and breathing with multiple periods can be observed, eventually becoming chaotic. In all of these cases, the dark pulse KFC remains localized. In the gray region, however, dark pulse KFCs lose stability to chaotic but transient oscillations, and eventually collapse to the HSS. More details about these dynamics and a more elaborate bifurcation analysis will be presented in [35].

In summary, we have provided a bifurcation analysis of dark pulse KFCs and mapped out their existence and stability conditions, as well as some of their dynamical instabilities. The KFCs are shown to be organized in a collapsed snaking structure resulting from the oscillatory tails of the SW that form them. Many observed properties of dark pulse KFCs, including coexistence of dark structures of different widths, can be similarly explained based on known features of SW dynamics. We note that MI, despite occurring in normal GVD resonators [36], does not play a crucial role in this description: the SWs connect the upper and lower HSSs and are not related to extended patterns. Some form of MI involving different microresonator mode families is, however, likely to be involved in explaining the soft excitation of dark pulse KFCs [18, 21].

We acknowledge support from the Research Foundation–Flanders (FWO-Vlaanderen) (PPR), the KU Leuven Junior Mobility Programme (LG), the Belgian Science Policy Office (BelSPO) under Grant IAP 7-35, the Research Council of the Vrije Universiteit Brussel, the Spanish MINECO and FEDER under Grant Intense@Cosyp (FIS2012-30634) (DG), the National Science Foundation under grant DMS-1211953 (EK), and the Marsden Fund of the Royal Society of New Zealand (SC). We also thank F. Leo for valuable discussions.

[1] P. Del'Haye, A. Schliesser, O. Arcizet, T. Wilken, R. Holzwarth, and T. J. Kippenberg, "Optical frequency comb generation from a monolithic microresonator," Nature **450**, 1214–1217 (2007).

[2] T. J. Kippenberg, R. Holzwarth, and S. A. Diddams, "Microresonator-based optical frequency combs," Science

332, 555–559 (2011).
[3] Y. Okawachi, K. Saha, J. S. Levy, Y. H. Wen, M. Lipson, and A. L. Gaeta, "Octave-spanning frequency comb generation in a silicon nitride chip," Opt. Lett. **36**, 3398–3400 (2011).
[4] S. B. Papp, K. Beha, P. Del'Haye, F. Quinlan, H. Lee, K. J. Vahala, and S. A. Diddams, "Microresonator frequency comb optical clock," Optica **1**, 10–14 (2014).
[5] F. Ferdous, H. Miao, D. E. Leaird, K. Srinivasan, J. Wang, L. Chen, L. T. Varghese, and A. M. Weiner, "Spectral line-by-line pulse shaping of on-chip microresonator frequency combs," Nature Photon. **5**, 770–776 (2011).
[6] T. Herr, K. Hartinger, J. Riemensberger, C. Y. Wang, E. Gavartin, R. Holzwarth, M. L. Gorodetsky, and T. J. Kippenberg, "Universal formation dynamics and noise of Kerr-frequency combs in microresonators," Nature Photon. **6**, 480–487 (2012).
[7] J. Pfeifle, V. Brasch, M. Lauermann, Y. Yu, D. Wegner, T. Herr, K. Hartinger, P. Schindler, J. Li, D. Hillerkuss, R. Schmogrow, C. Weimann, R. Holzwarth, W. Freude, J. Leuthold, T. J. Kippenberg, and C. Koos, "Coherent terabit communications with microresonator Kerr frequency combs," Nature Photon. **8**, 375–380 (2014).
[8] F. Leo, S. Coen, P. Kockaert, S.-P. Gorza, Ph. Emplit, and M. Haelterman, "Temporal cavity solitons in one-dimensional Kerr media as bits in an all-optical buffer," Nature Photon. **4**, 471–476 (2010).
[9] S. Coen, H. G. Randle, T. Sylvestre, and M. Erkintalo, "Modeling of octave-spanning Kerr frequency combs using a generalized mean-field Lugiato-Lefever model," Opt. Lett. **38**, 37–39 (2013).
[10] F. Leo, L. Gelens, Ph. Emplit, M. Haelterman, and S. Coen, "Dynamics of one-dimensional Kerr cavity solitons," Opt. Express **21**, 9180–9191 (2013).
[11] S. Coen and M. Erkintalo, "Universal scaling laws of Kerr frequency combs," Opt. Lett. **38**, 1790–1792 (2013).
[12] T. Herr, V. Brasch, J. D. Jost, C. Y. Wang, N. M. Kondratiev, M. L. Gorodetsky, and T. J. Kippenberg, "Temporal solitons in optical microresonators," Nature Photon. **8**, 145–152 (2014).
[13] P. Parra-Rivas, D. Gomila, M. A. Matías, S. Coen, and L. Gelens, "Dynamics of localized and patterned structures in the Lugiato-Lefever equation determine the stability and shape of optical frequency combs," Phys. Rev. A **89**, 043813 (2014).
[14] C. Godey, I. V. Balakireva, A. Coillet, and Y. K. Chembo, "Stability analysis of the spatiotemporal Lugiato-Lefever model for Kerr optical frequency combs in the anomalous and normal dispersion regimes," Phys. Rev. A **89**, 063814 (2014).
[15] Y. K. Chembo and C. R. Menyuk, "Spatiotemporal Lugiato-Lefever formalism for Kerr-comb generation in whispering-gallery-mode resonators," Phys. Rev. A **87**, 053852 (2013).
[16] W. Liang, A. A. Savchenkov, V. S. Ilchenko, D. Eliyahu, D. Seidel, A. B. Matsko, and L. Maleki, "Generation of a coherent near-infrared Kerr frequency comb in a monolithic microresonator with normal GVD," Opt. Lett. **39**, 2920–2923 (2014).
[17] S.-W. Huang, H. Zhou, J. Yang, J. F. McMillan, A. Matsko, M. Yu, D.-L. Kwong, L. Maleki, and C. W. Wong, "Mode-locked ultrashort pulse generation from on-chip normal dispersion microresonators," Phys. Rev. Lett. **114**, 053901 (2015).
[18] X. Xue, Y. Xuan, Y. Liu, P.-H. Wang, S. Chen, J. Wang, D. E. Leaird, M. Qi, and A. M. Weiner, "Mode-locked dark pulse Kerr combs in normal-dispersion microresonators," Nature Photon. **9**, 594–600 (2015).
[19] A. B. Matsko, A. A. Savchenkov, and L. Maleki, "Normal group-velocity dispersion Kerr frequency comb," Opt. Lett. **37**, 43–45 (2012).
[20] A. Coillet, I. Balakireva, R. Henriet, K. Saleh, L. Larger, J. Dudley, C. Menyuk, and Y. Chembo, "Azimuthal turing patterns, bright and dark cavity solitons in Kerr combs generated with whispering-gallery-mode resonators," IEEE Photonics Journal **5**, 6100409 (2013).
[21] V. E. Lobanov, G. Lihachev, T. J. Kippenberg, and M. L. Gorodetsky, "Frequency combs and platicons in optical microresonators with normal GVD," Opt. Express **23**, 7713–7721 (2015).
[22] N. N. Rozanov, V. E. Semenov, and G. V. Khodova, "Transverse structure of a field in nonlinear bistable interferometers. i. switching waves and steady-state profiles," Sov. J. Quantum. Electron. **12**, 193–197 (1982).
[23] S. Coen, M. Tlidi, Ph. Emplit, and M. Haelterman, "Convection versus dispersion in optical bistability," Phys. Rev. Lett. **83**, 2328–2331 (1999).
[24] L. A. Lugiato and R. Lefever, "Spatial dissipative structures in passive optical systems," Phys. Rev. Lett. **58**, 2209–2211 (1987).
[25] M. Haelterman, S. Trillo, and S. Wabnitz, "Additive-modulation-instability ring laser in the normal dispersion regime of a fiber," Opt. Lett. **17**, 745–747 (1992).
[26] M. Tlidi and L. Gelens, "High-order dispersion stabilizes dark dissipative solitons in all-fiber cavities," Opt. Lett. **35**, 306–308 (2010).
[27] Y. Pomeau, "Front motion, metastability and subcritical bifurcations in hydrodynamics," Physica D **23**, 3–11 (1986).
[28] P. Colet, M. A. Matías, L. Gelens, and D. Gomila, "Formation of localized structures in bistable systems through nonlocal spatial coupling. I. general framework," Phys. Rev. E **89**, 012914 (2014).
[29] L. Gelens, M. A. Matías, D. Gomila, T. Dorissen, and P. Colet, "Formation of localized structures in bistable systems through nonlocal spatial coupling. II. the nonlocal ginzburg-landau equation," Phys. Rev. E **89**, 012915 (2014).
[30] B. A. Malomed, "Bound states of envelope solitons," Phys. Rev. E **47**, 2874–2880 (1993).
[31] B. Schäpers, M. Feldmann, T. Ackemann, and W. Lange, "Interaction of localized structures in an optical pattern-forming system," Phys. Rev. Lett. **85**, 748–751 (2000).
[32] I. V. Barashenkov, S. R. Woodford, and E. V. Zemlyanaya, "Interactions of parametrically driven dark solitons. i. néel-néel and bloch-bloch interactions," Phys. Rev. E **75**, 026604 (2007).
[33] Y.-P. Ma and E. Knobloch, "Depinning, front motion, and phase slips," Chaos **22**, 033101 (2012).
[34] E. Knobloch, "Spatial localization in dissipative systems," Annu. Rev. Cond. Mat. Phys. **6**, 325–359 (2015).
[35] P. Parra-Rivas, D. Gomila, E. Knobloch, and L. Gelens "Dark solitons in the Lugiato-Lefever equation with normal dispersion," (in preparation).
[36] S. Coen and M. Haelterman, "Competition between modulational instability and switching in optical bistability," Opt. Lett. **24**, 80–82 (1999).